

# Supporting information

## A bulk effect-free method for binding kinetic measurements enabling small molecule affinity characterization

Allison M. Marn,<sup>\*,†</sup> Elisa Chiodi,<sup>†</sup> and M. Selim Ünlü<sup>†,‡</sup>

<sup>†</sup>*Department of Electrical and Computer Engineering, Boston University, Boston (MA)*

<sup>‡</sup>*Department of Biomedical Engineering, Boston University, Boston (MA)*

E-mail: ammarn@bu.edu

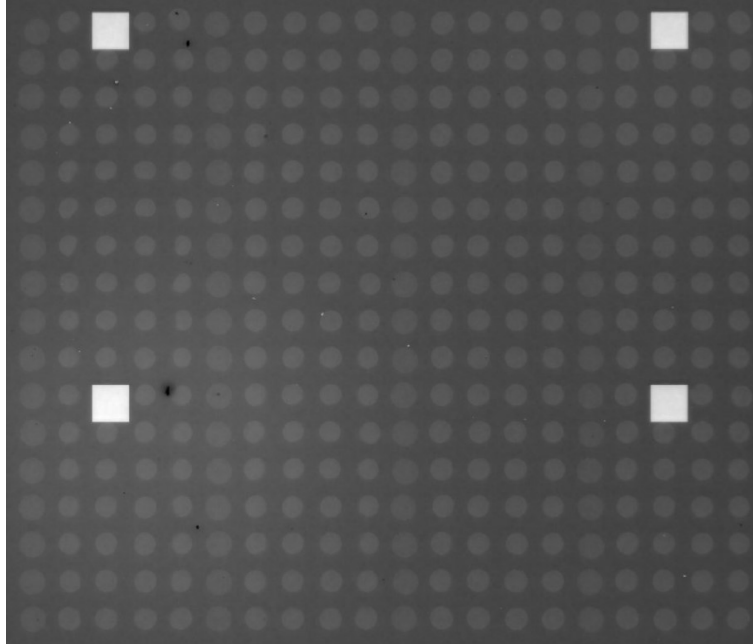


Figure S1: IRIS image of the one of the chips used for the experiments. The chip contains a repeating pattern of four rows of streptavidin molecules, deposited at a spotting concentration of  $18\mu M$  followed by one row of Bovine Serum Albumin (BSA), spotted as a negative control at a spotting concentration of  $15\mu M$ .

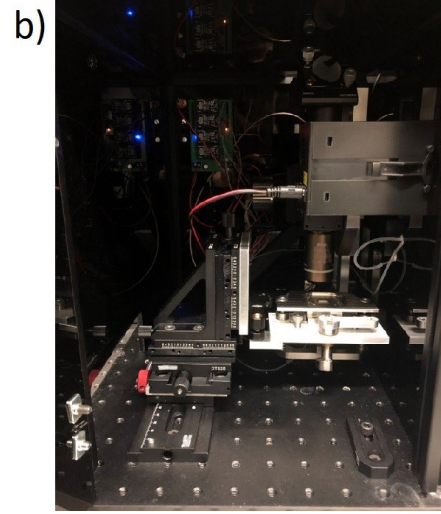
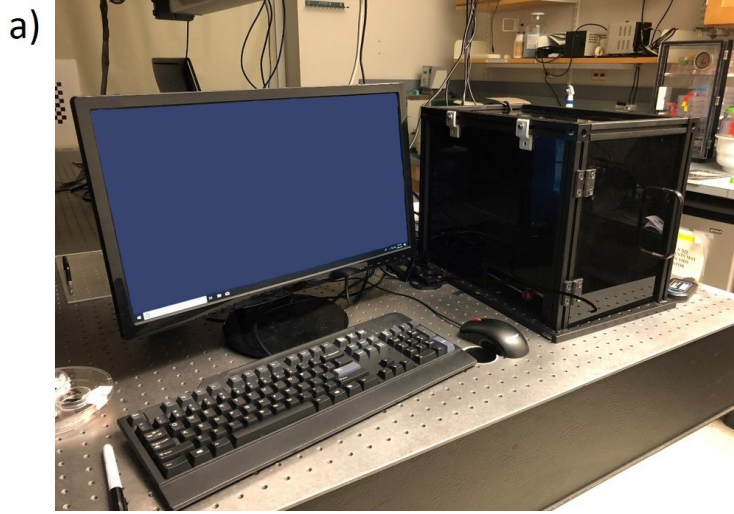


Figure S2: Picture of the a) external IRIS benchtop device and b) the internal view of the system.

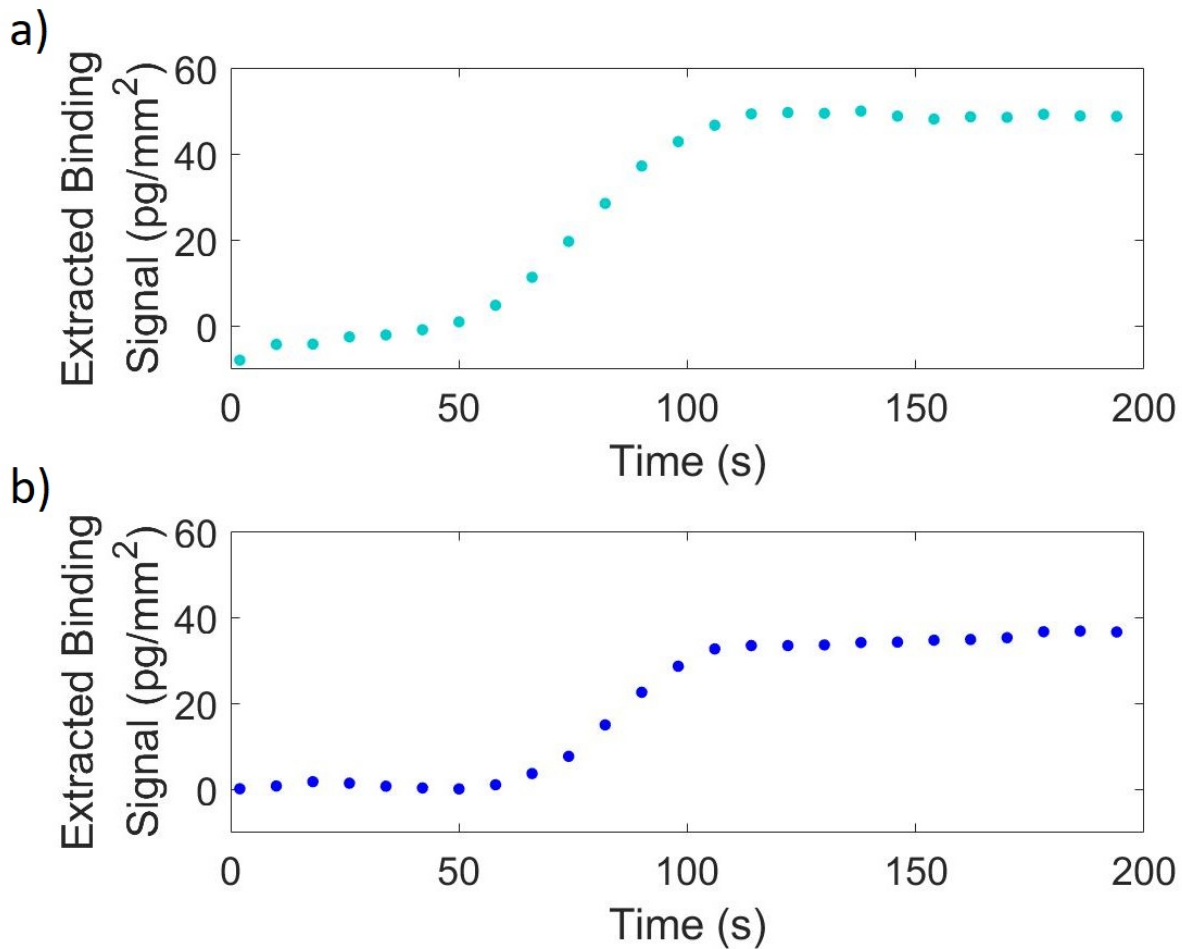


Figure S3: a) Binding curve for  $1\mu\text{M}$  biotin in 1%DMSO in PBS to immobilized streptavidin, with PBS as the buffer solution, using illumination engineering to correct for the bulk effect. b) Binding curve for  $1\mu\text{M}$  biotin in 1%DMSO in PBS to immobilized streptavidin when 1%DMSO in PBS is used as the both the buffer and the sample solution media (no bulk refractive index difference between solutions), and acquisition was done using a single color illumination (420nm blue LED). The curve has the same appearance in both cases.

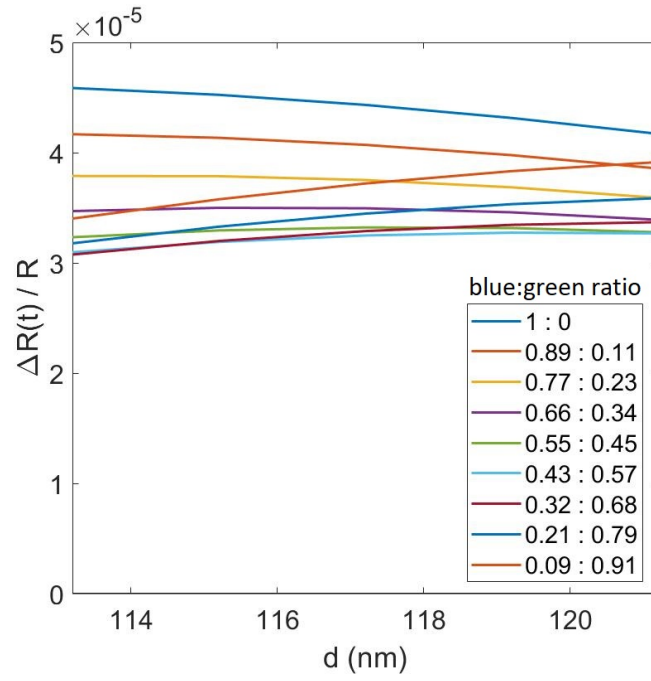


Figure S4: The reflectivity response of various ratios of blue:green dual illumination across the range of thicknesses where the proposed bulk effect elimination method is possible.

# 1 Biotin-Streptavidin Interaction: Mass Transport Limitation

At a  $1\mu\text{M}$  concentration, biotin binds effectively immediately to streptavidin due to their high binding affinity ( $K_d=10^{-15}$ ). Figure S5 shows the simulated binding curves for biotin concentrations of  $1\mu\text{M}$ ,  $1\text{nM}$ , and  $1\text{pM}$ , while Figure S6 shows the actual measured binding curves for these concentrations. A high concentration of biotin is needed for enough molecules to be accessible to the surface molecules to observe binding in a timely manner. The system used for these experiments captures a data point every 6 seconds. Under ideal conditions, where sufficient molecules are introduced to the immobilized streptavidin, the binding curve would reach saturation after one data point, following the simulated behavior. As this does not, it is apparent that adequate molecules are not accessible by the streptavidin molecules for binding.

The limitation can be understood by examining the experiments performed from the standpoint of a theoretical model. Streptavidin can be modeled as a  $4.66\text{nm}$  diameter sphere with each streptavidin molecule having 4 biotin binding sites<sup>1</sup>. Assuming a  $200\mu\text{m}$  spot size and a monolayer of streptavidin, there would be  $\sim 4.6 \times 10^8$  streptavidin molecules ( $\sim 1.8 \times 10^9$  binding sites) immobilized on the sensor in one spot. A cross sectional of the sensor containing one row of 17 spots, therefore, contains  $\sim 3.1 \times 10^{10}$  binding sites. The  $1\mu\text{M}$  biotin solution flowing at  $200\mu\text{L}/\text{min}$  means that  $\sim 2 \times 10^{12}$  molecules per second at flowing through any cross section, supplying plenty of molecules to saturate the streptavidin binding sites within 1 second, though the measured binding is on a much slower scale. With sufficient molecules available in the volume, the problem remains that these molecules are not able to diffuse to be in close enough proximity to bind at the expected kinetic rate, implying mass transport limitation<sup>2</sup>.

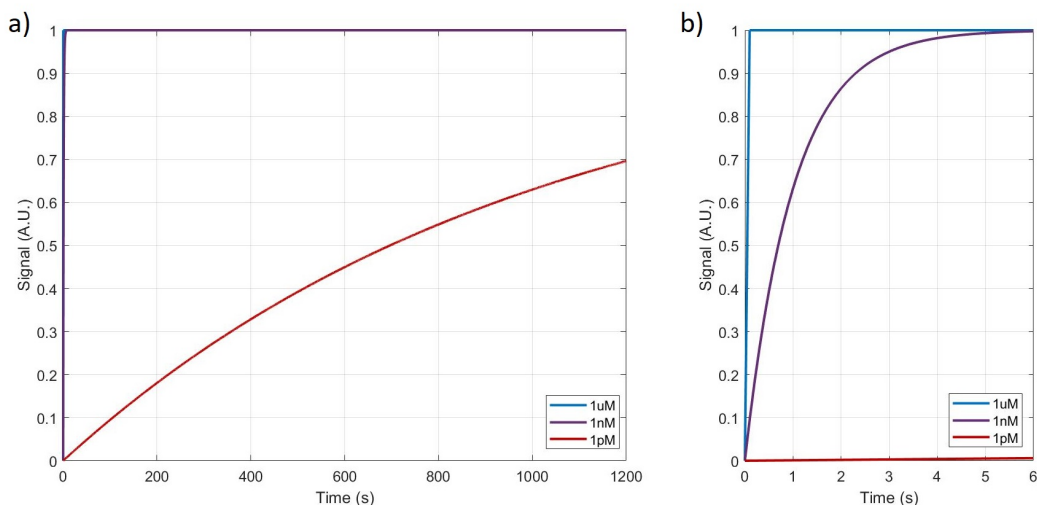


Figure S5: Simulated binding curves for biotin against immobilized streptavidin for concentrations of  $1\mu\text{M}$ ,  $1\text{nM}$ , and  $1\text{pM}$  over a) 1200 seconds and b) over 6 seconds.

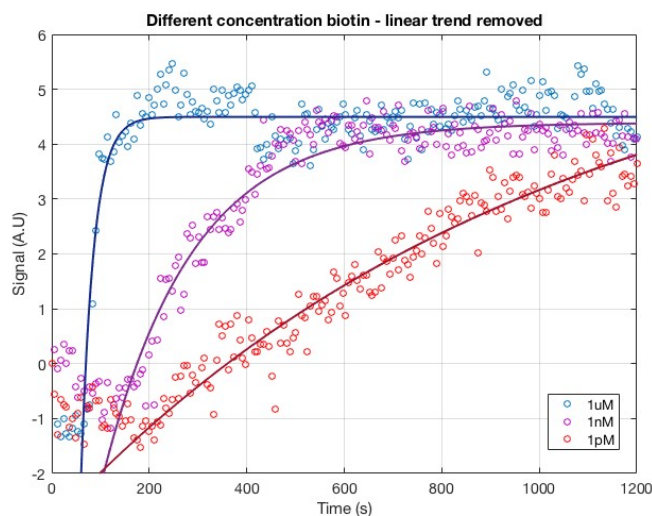


Figure S6: Measured binding curves for biotin against immobilized streptavidin for concentrations of  $1\mu\text{M}$ ,  $1\text{nM}$ , and  $1\text{pM}$ . The curves are fitted with a 1:1 Langmuir model. Each curve is the average of 42  $120\mu\text{m}$ -diameter streptavidin spots, at a spotting concentration of  $1\text{mg}/\text{mL}$ .

## 2 The Evolution of IRIS Measurements

The information on biomass thickness and accumulation for performing these binding kinetic measurements is encoded in the spectral signature of interferometric reflectivity; the task is then in extracting this information. In the first implementation of IRIS, white

light illumination and a spectrometer were used to capture the reflectance spectrum.<sup>3</sup> The reflected white light interference from a layered substrate resulted in periodic oscillations in the reflection spectrum. The reflection spectrum was then used to calculate relative changes in thickness. The white light source was then replaced with a LED source, though still using a spectrometer to capture the periodic oscillations in the reflection spectrum to calculate the film thickness.<sup>4</sup>

However, a spectrometer is single-point detection method, which severely limited the throughput of the system. The single-point measurement spectrometer was replaced with a CCD camera with 250,000 pixels, allowing for multiplexed measurements without the additional time and hardware needed to scan the sample.<sup>5</sup> With a CCD camera to measure intensity, a tunable laser was used to generate the reflectance spectrum at 1nm steps from 764nm to 784nm.

While the imaging modality offered vast improvement in multiplexing, tunable lasers are expensive and delicate, and the wavelength step size was much more than was needed to generate the spectral reflectance curve. The tunable laser source was therefore replaced with four discrete LED sources to generate the reflectance curve.<sup>6</sup> Images were captured with each of the four LEDs at every time point for the duration of the experiment, The four LED wavelength data for each pixel at every time point were used to fit a reflectance curve and extract the biofilm thickness information. While sensitive and simple in implementation, the process was computationally heavy resulting in a length analysis time. In the current implementation of IRIS, images captured with each of four LEDs, along with the LED spectra information, are used to fit the data to a spectral reflectance curve and calculate the film thickness. Sevenler et al. demonstrated that capturing these four images as an initial calibration measurement could be used to generate a look up table for converting measured changes in intensity to biomass accumulation values based on the spectral reflectance curve.<sup>7</sup> The implementation of the lookup table allowed for the same sensitivity and a 10,000 fold improvement in analysis time.



IRIS continues to leverage the spectral signature of interferometric reflectivity for sensitive biomass measurements, though the methodology has evolved over a decade. The multiplexed, highly sensitive, method now captures the spectral information using a single time point four image spectrum, captured with a CMOS camera in each of four LED illuminations, allowing for the conversion of subsequent images from intensity to biomass.

## References

- (1) Chiodi, E.; Marn, A. M.; Geib, M. T.; Ekiz Kanik, F.; Rejman, J.; AnKrapp, D.; Ünlü, M. S. Highly Multiplexed Label-Free Imaging Sensor for Accurate Quantification of Small-Molecule Binding Kinetics. *ACS Omega* **2020**, *5*, 25358–25364.
- (2) Squires, T. M.; Messinger, R. J.; Manalis, S. R. Making it stick: convection, reaction and diffusion in surface-based biosensors. *Nat Biotech* **2008**, *26*, 417–426.
- (3) Moiseev, L.; Ünlü, M. S.; Swan, A. K.; Goldberg, B. B.; Cantor, C. R. DNA conformation on surfaces measured by fluorescence self-interference. *Proc. Natl. Acad. Sci.* **2006**, *103*, 2623–2628.
- (4) Zhang, X.; Daaboul, G. G.; Spuhler, P. S.; Freedman, D. S.; Yurt, A.; Ahn, S.; Avcı, O.; Ünlü, M. S. Nanoscale characterization of DNA conformation using dual-color fluorescence axial localization and label-free biosensing. *Analyst* **2014**, *139*, 6440–6449.
- (5) Özkumur, E.; Yalçın, A.; Cretich, M.; Lopez, C. A.; Bergstein, D. A.; Goldberg, B. B.; Chiari, M.; Ünlü, M. S. Quantification of DNA and protein adsorption by optical phase shift. *Biosens. Bioelectron.* **2009**, *25*, 167 – 172.
- (6) Daaboul, G.; Vedula, R.; Ahn, S.; Lopez, C.; Reddington, A.; Ozkumur, E.; Ünlü, M. LED-based Interferometric Reflectance Imaging Sensor for quantitative dynamic monitoring of biomolecular interactions. *Biosens. Bioelectron.* **2011**, *26*, 2221 – 2227.

- (7) Sevenler, D.; Selim Unlu, M. Numerical techniques for high-throughput reflectance interference biosensing. *J. Mod. Opt.* **2016**, *63*, 1115–1120.